Journal of Applied Electrochemistry **31**: 671–676, 2001.

Steady-state mass transport at stationary discs under divergent laminar radial flow conditions

F. CŒURET[1]* and T.Z. FAHIDY[2]
[1]*Laboratoire de Thermocinétique, UMR CNRS 6607-Nantes, implantation Ecole Louis de Broglie, Campus de Ker Lann, 35170 Bruz, France*
[2]*Department of Chemical Engineering, University of Waterloo, Waterloo, ON N2L3G1, Canada*
*(*author for correspondence, e-mail: coeuret@isitem.univ-nantes.fr)*

Received 8 June 2000; accepted in revised form 3 January 2001

Key words: electrochemical reactor, laminar radial flow, mass transfer

Abstract

This paper deals with global and local wall-to-liquid mass transfer under divergent laminar radial flow conditions between two parallel stationary discs. Approximate theoretical expressions for local and overall transport rates in piston flow and Poiseuille flow, and empirical correlations from the literature, are compared to experimental observations utilizing the electrochemical method of rate measurement. The experimental results support the theoretical approach for this laminar flow regime, the latter expanding the scope of the applicability of electrochemical methods presented in the literature.

List of symbols

a	half thickness of the interdisc gap (m)
C	concentration (mol m^{-3})
C^*	dimensionless concentration
C_E	entrance concentration, at $r = R_1$ (mol m^{-3})
C_S	exit concentration, at $r = R_2$ (mol m^{-3})
C_i	concentration at the mass transfer surface (mol m^{-3})
$\overline{C}(x^*)$	mean bulk concentration at x^* (mol m^{-3})
D	molecular diffusion coefficient (m^2 s^{-1})
$f(y^*)$	dimensionless velocity function
I_L	limiting diffusion current (A)
$I_L(r)$	local limiting diffusion current, at r (A)
$k_d(r)$	local mass transfer coefficient at r (m s^{-1})
$k_d(x^*)$	local mass transfer coefficient (m s^{-1})
$\overline{k_d}$	mean mass transfer coefficient (m s^{-1})
Nu	Nusselt number
Pr	Prandtl number
Q_v	volumetric flow rate of the fluid (m^3 s^{-1})
R_1	inner radius (m)
R_2	outer radius (m)
Re	Reynolds number, $(Q_V/(4\pi a v))$
r	radial coordinate (m)
r_c	critical radial coordinate (m)
Sc	Schmidt number, (v/D)
$Sh(x^*)$	local Sherwood number for x^*
$\overline{Sh}$	mean Sherwood number between $r = R_1$ and $r = R_2$, $(2a\overline{k_d}/D)$
x^*	dimensionless distance parameter, $((r^2 - {R_1}^2)/(2\ Re\ Sc\ a^2))$
y	distance coordinate in the gap
y^*	dimensionless coordinate in the gap, (y/a)

Greek symbols

v	kinematic viscosity (m^2 s^{-1})

Subscripts

1	at $r = R_1$
2	at $r = R_2$

1. Introduction

The advent of the capillary gap cell [1] and the pump cell [2] in industrial electrochemistry has amply demonstrated the importance of mass transport in divergent laminar radial flow. As shown in a recent experimental study [3], several experimental works were concerned with the problem, and a graphical comparison of empirical correlations available for steady-state mass transport rates at the liquid–solid disc interface was presented. Dworak and Wendt [4] gave a rigourous theoretical solution of the mass transfer problem in relation to the hydrodynamics within the capillary gap cell. With the exception of their work, the development of mass transfer relationships has relied largely on abundant heat transfer studies in the literature.

An essential fact is the tendency of laminar piston flow originating at the entry location to assume a parabolic profile, as the mean radial fluid velocity decreases with radial distance, past a certain value of

the radial coordinate. There exists, therefore, a spatial domain where piston-flow and parabolic (i.e., Poiseuille) flow coexist with obvious implications for mass transport. This is the reason why both cases of piston flow and of Poiseuille flow were considered separately in theoretical studies.

Major references in this field are the contributions of Thomas and Cobble [5] and Kreith [6–8], the latter being generally considered cornerstone publications. Kreith established appropriate dimensionless relationships between the Nusselt number, *Nu*, and the dimensionless parameter, x_2^*, comprising geometric properties and dimensionless numbers *Re* (Reynolds number) and *Pr* (Prandtl number). More recently, Mochizuki and Yao [8] obtained a numerical solution for the case of constant heat flux at one of the discs, along with experimental measurements; they demonstrated the effect of flow separation on transport characteristics. Cavalcanti and Cœuret [3] studied mass transport experimentally with particular emphasis on the effect of limited geometrical and hydrodynamic conditions. Results presented in the current paper extend the experimental scope of [3] and provide grounds for comparison with empirical findings in the literature, and with approximate theoretical solutions.

2. Theory

2.1. *Problem definition*

Steady-state mass transfer between a disc and a liquid in radially diverging laminar flow between two circular stationary discs separated by a distance $2a \ll R_2$ (Figure 1), is governed by the convective diffusion equation:

$$\frac{\partial^2 C^*}{\partial y^{*2}} = f(y^*)\frac{\partial C^*}{\partial x^*} \tag{1}$$

where:

$$C^* \equiv C^*(x^*, y^*) \equiv \frac{C - C_i}{C_E - C_i}$$

$$x^* \equiv \frac{r^2 - R_1^2}{2Re\,Sc\,a^2}; \quad y^* \equiv \frac{y}{a}$$

are dimensionless variables in which *Re* and *Sc* are the Reynolds number and the Schmidt number, respectively, and $f(y^*)$ represents the dimensionless velocity profile between the two parallel discs ($f(y^*) = 1$ in piston flow and $f(y^*) = 3(1 - y^{*2})/2$ in Poiseuille flow). If a constant concentration is maintained at one of the two disc surfaces, the problem is similar to heat transfer between a flowing liquid and one disc held at a constant temperature, while the second disc is isolated. In this configuration, the boundary conditions are as follows:

$$C^*(0, y^*) = 1$$

$$C^*(x^*, -1) = 0$$

The local mass transport coefficient may be written as

$$k_d(x^*) = k_d(r) = -\frac{D}{\overline{C}(x^*) - C_i}\left(\frac{\partial C}{\partial y}\right)_{y=-a} = -\frac{DC_E - C_i}{aC(x^*) - C_i}\left(\frac{\partial C^*}{\partial y^*}\right)_{y^*=-1}$$

where $\overline{C}(x^*)$ is the bulk concentration at x^*. The mean mass transport coefficient is then obtained as

$$\overline{k_d} = \frac{1}{\pi(R_2^2 - R_1^2)}\int_{R_1}^{R_2}(2\pi r)k_d(r)\mathrm{d}r = \frac{1}{x_2^*}\int_0^{x_2^*} k_d(x^{*2})\mathrm{d}x^*$$

from which $Sh(x^*)$ and $\overline{Sh}$ can readily be computed.

2.2. *Approximate solutions*

Although an exact solution of Equation 1 may be attempted on the basis of heat transfer theory, the fact that $Sc \gg Pr$ in aqueous solutions permits significant simplifications of practical value. In the case of Poiseuille flow, Dworak and Wendt [4] obtained a rigorous but complex solution for the concentration profile; they also obtained an approximate expression for $k_d(r)$, assuming that the concentration change is localized within a thin

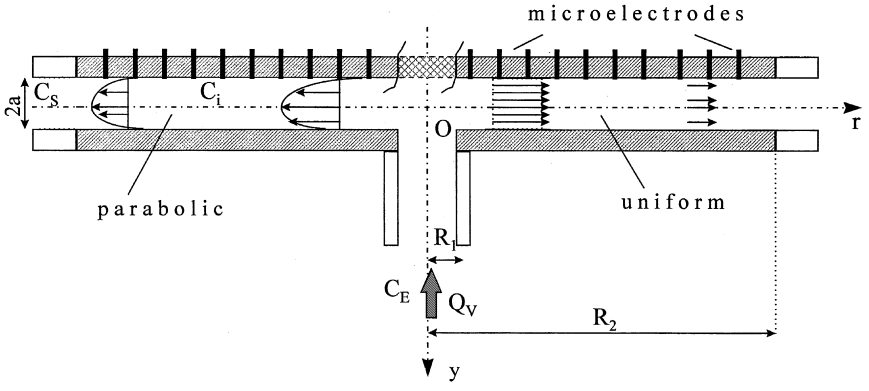

Fig. 1. Schematic view of the apparatus and the two possibilities of laminar flow.

boundary layer. For the latter, it follows from their results that:

$$Sh(x^*) = \left\{ \frac{4\pi a^2 Re\, Sc}{2Re\, Sc\, a^2\, x^* + R_1^2} \right\}^{1/3} \tag{2}$$

whose integration between $r = R_1$ and $r = R_2$, (i.e., between 0 and x_2^*) leads to

$$\overline{Sh} = 2.49\,\pi^{1/3}\,\frac{(R_2^2 - R_1^2)^{1/3}(R_2^{1/3} - R_1^{1/3})}{R_2 - R_1}\,\frac{1}{(x_2^*)^{1/3}} \tag{3}$$

Other approximate solutions can be obtained for the case of zero conversion through the cell ($\overline{C}(x^*) = C_E = \text{const.}$). If a negligible penetration depth (i.e., a negligible thickness of the concentration layer at the wall) is assumed (this is a standard case in chemical engineering) specifically:

(i) In piston flow, the solution of Equation 1 can be adapted from the known solution for unsteady diffusional mass transport or heat conduction into a semiinfinite medium [10], to yield:

$$k_d(x^*) = \frac{D}{a\sqrt{\pi}}\,\frac{1}{(x^*)^{1/2}}$$

or

$$Sh(x^*) = \frac{2}{\sqrt{\pi}}\,\frac{1}{(x^*)^{1/2}} \tag{4a}$$

and consequently, under global conditions:

$$\overline{k_d} = \frac{1}{x_2^*}\int_0^{x_2^*} k_d(x^*)\mathrm{d}x^* = \frac{2D}{a\sqrt{\pi}}\,\frac{1}{(x_2^*)^{1/2}}$$

or

$$\overline{Sh} = \sqrt{\frac{32}{\pi}}\,\frac{1}{(2x_2^*)^{1/2}} \tag{4b}$$

(ii) In Poiseuille flow, considering that near the wall the radial velocity is proportional to y^*, the problem is similar to the dissolution of a solid into a vertical laminar falling film at short contact times [11]. The adapted solution yields:

$$Sh(x^*) = 1.553\,\frac{1}{(x_2^*)^{1/3}} \tag{5a}$$

$$\overline{Sh} = 2.935\,\frac{1}{(2x_2^*)^{1/3}} \tag{5b}$$

In the limiting case where $R_1 \ll R_2$, Equation 3 simplifies to Equation 5b but with a multiplyer of 4.59 in place of 2.935.

3. Experimental details

The Altuglas experimental cell, shown in Figure 2, was the same as that employed in an earlier investigation [3]. The two nickel discs having a diameter of 9 cm were inserted in PVC rings and threaded into supporting frames. The liquid entered the lower disc through a 0.6 cm diameter orifice, flowed along the radial coordinate, and left the cell at the top. The upper disc portion facing the inlet orifice was nonconducting over a circular area of 6 mm radius.

The liquid was pumped from a storage reservoir by a peristaltic pump to a level held constant in a second reservoir. The inlet rate Q_V to the cell was controlled by two valves, and its magnitude (0.3–35 $\mathrm{dm^3\ h^{-1}}$) was measured by mass at the discharge end. The mass transport rates were measured electrochemically [12] using an 0.5 M aqueous NaOH solution containing a mixture of 0.005 M $Fe(CN)_6K_3$ and 0.05 M $Fe(CN)_6K_4$.

The lower disc served as the anode, and the upper (cathode) disc contained 400 μm diameter nickel-thread microelectrodes sealed with special Araldite into 600 μm diameter perforations. Separated by a 5 mm distance from one another, the microelectrodes were used to measure limiting currents locally along a diameter of the upper disc radius. When overall currents were measured, one of the microelectrodes was chosen as redox reference electrode, while for the measurement of local currents the microelectrode placed immediately next to the studied microelectrode served this purpose.

All experiments were carried out at 20 °C, where the ferricyanide diffusion coefficient, measured via a rotating disc, was found to be $D = 5.55 \times 10^{-10}\ \mathrm{m^2\ s^{-1}}$. The kinematic viscosity was $v = 1.021 \times 10^{-6}\ \mathrm{m^2\ s^{-1}}$; thus $Sc = 1846$.

The electrical set-up consisted of a Tacussel PRT 20-2X potentiostat with a Tacussel Pilovit–NUM control unit, and a two channel Sefram–Servotrace recorder to obtain potential against time curves. The overall current was measured in the anode circuit as a potential drop across a 1 ohm shunt resistance, whereas the local current at a given microelectrode was obtained as a

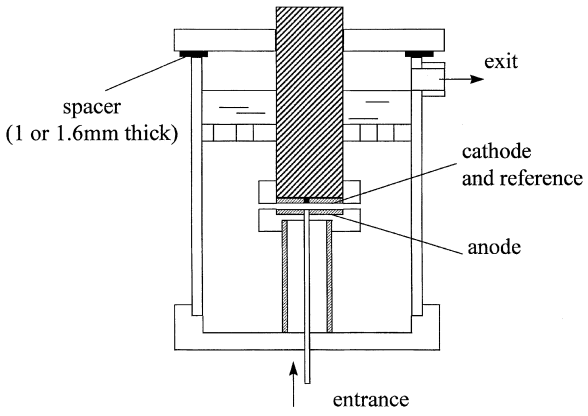

Fig. 2. Experimental cell.

potential drop over a 200 ohm shunt resistance connected in series with the microelectrode.

The disc surfaces, including the microelectrodes, were polished mechanically to 0.25 μm, and activated chemically by a 50% hydrochloric acid solution over 30 s. The separation distance between the discs had two values (1 mm and 1.6 mm).

4. Results

4.1. *Experimental observations*

The global limiting current I_L increases rapidly at small values of the volumetric flow rate Q_V (Figure 3), but the rate of increase becomes smaller and approximately linear past about 10 $dm^3\ h^{-1}$. At $2a = 1$ mm, the experimental Re varies between 16 and 1340; at $2a = 1.6$ mm, the Re range is 36–1300. In the latter case, and at $Re = 1300$, fluctuations in I_L have been observed, in contrast with the $2a = 1$ mm, $Re = 1300$ case. It appears, therefore, that in agreement with Ishizawa [13], the $Re\,(a/R_1)^2$ product characterizes the flow effect better than Re; this quantity $Re\,(a/R_1)$ is contained in the dimensionless number x^* introduced in earlier work via dimensional consistency considerations [3] for Equation 1.

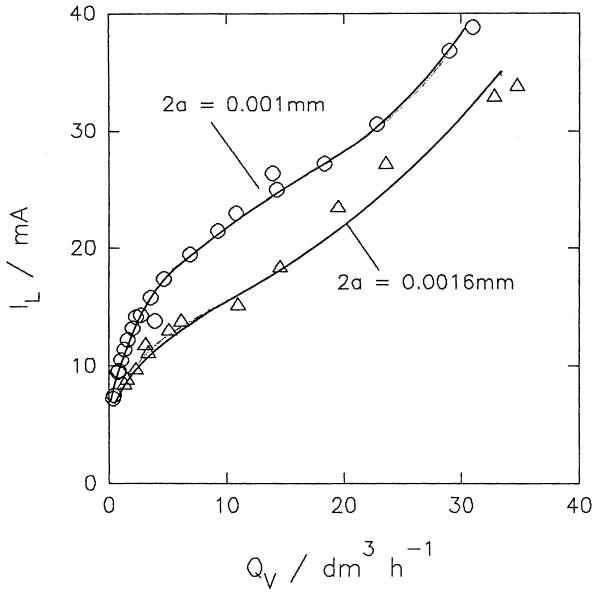

Fig. 3. Experimentally observed variation of the limiting current I_L with the volumetric flow rate Q_V.

The local limiting currents (obtained over 1.257×10^{-7} m^2 microelectrode areas) vary with the radial coordinate, as shown in Figures 4 and 5. In the case of $2a = 1$ mm, $I_L(r)$ decreases monotonically with r at low values of Re (Figure 4(a); $Re < 840$), but at $Re = 840$ a local minimum and a local maximum are observed at about $r = 11$ and $r = 13$ mm, respectively (Figure 4(b)). At $2a = 1.6$ mm (Figure 5) the appearance of local extrema becomes quite pronounced at $Re = 530$ and $Re = 945$, but in the latter case, the local current is also fluctuating.

4.2. *Analysis of global phenomena*

Due to the electrochemical system which consumes ferricyanide at the cathode and produces the same amount of it at the anode, the mean ferricyanide concentration remains constant through the cell channel. In other words, because of laminar flow between relatively small discs, the diffusion boundary layer at the cathode is separated from the corresponding layer for ferricyanide at the anode, in spite of the close vicinity of the discs. It is instructive to note that Dworak and Wendt [4] also used the electrochemical reduction of ferricyanide, but from a solution free of ferrocyanide, in a cell with discs larger ($R_1 = 3$ cm; $R_2 = 15$ cm) than in the current work and very small gaps ($2a = 0.02$ cm or

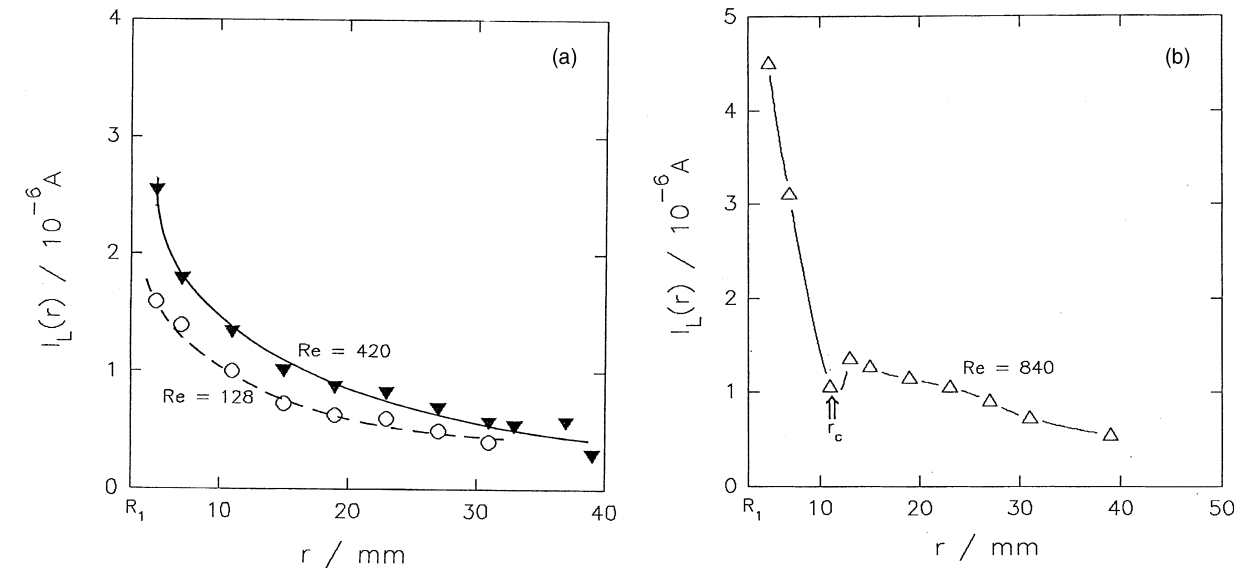

Fig. 4. Radial distribution of the current, measured by a set of microelectrodes ($2a = 1.0$ mm). (a) $Re = 128$ and 420; (b) $Re = 840$.

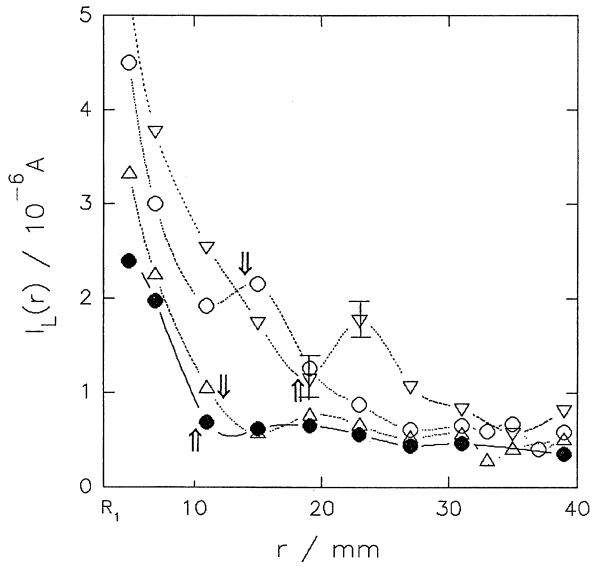

Fig. 5. Radial distribution of the current, measured by a set of microelectrodes ($2a$ = 1.6 mm). *Re*: (●) 294, (△) 398, (○) 530 and (▽) 945.

0.05 cm) between the electrodes. In their case, they established that the reverse reaction at the counter electrode can be ignored, provided that conversion does not exceed 30%. In our case, with the neglect of the anodic production of ferricyanide, a conversion less than 13% ($2a$ = 0.001 m) and 5% ($2a$ = 0.0016 m) is computed from the overall experimental currents.

Figure 6 compares experimental values of $\overline{Sh}$ against $1/(2x_2^*)$ with experimental findings of Cavalcanti and Cœuret [3] in the same cell, but over a wider range of experimental conditions. The empirical correlations taken from the literature were obtained in mass transfer studies applying the electrochemical method [1, 2, 14], and from the heat transfer work of Kreith [8]. Figure 6 also shows the approximate theoretical equations

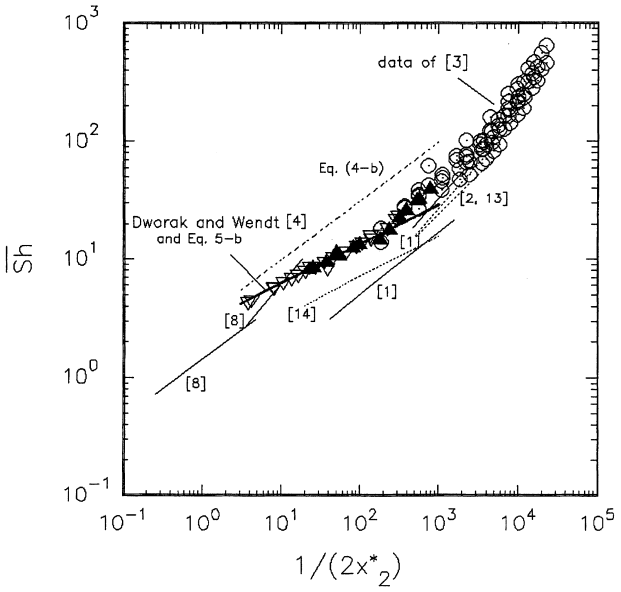

Fig. 6. Variation of the mean Sherwood number $\overline{Sh}$ with parameter $1/(2x_2^*)$. Key: (▽) this work ($2a$ = 1 mm); (▲) this work ($2a$ = 1.6 mm).

(Equations 3, 4b and 5b) and the approximation proposed by Shenoy and Fenton [15].

For the values of R_1 and R_2 of the present work, Equations 3 and 5b are essentially identical and they describe satisfactorily the results in the explored domain of laminar flow. This is an indication of the existence of a parabolic velocity profile in the cell channel. Equation 4b overestimates the experimental results.

4.3. *Analysis of local phenomena*

Figure 7 demonstrates that the experimental variation of local mass transport rates with dimensionless radial distance agrees in a satisfactory manner with the theoretical predictions of Equations 4a and 5a.

In computing the latter for the corresponding Reynolds numbers, the effect of conversion, 1% and 3% for $2a$ = 1 mm, and less than 1% for $2a$ = 1.6 mm, has been neglected and $C(x^*) \cong C_E$ was set. There is less scatter at $2a$ = 1 mm, although one would expect a slightly larger conversion than at $2a$ = 1.6 mm. As in the heat transport experiments by Mochizuki and Yao [9] in the absence of flow separation, the experimental points align themselves along a single curve positioned between the theoretical piston-flow and Poiseuille-flow model predictions.

5. Discussion

It is instructive to invoke heat transport-based observations of Mochizuki and Yao [9] with respect to Figures 4 and 5. These authors observed a monotonic decrease of $Nu(x^*)$ with increasing values of x^*, at low Reynolds numbers. At higher values of Re, the $Nu(x^*)$ curve exhibits a minimum followed by a maximum, similar to Figure 4(b). On the basis of flow visualization experiments, the existence of local extrema has been ascribed to flow separation from the solid surface at a certain radial position. There is theoretical evidence [16] for an inflexion point in the velocity profile at the surface past a critical radial distance $r_c = 0.76\ a\ Re^{1/2}$, which indicates flow instability. The arrows in Figures 4 and 5, denoting calculated values of r_c, are in to positions in the domain of the minimum/maximum sequence. The significance of the fluctuations appearing at Re = 945 (Figure 5) about r = 20 mm may well be an indication of vortices generated in the unstable flow region where turbulent flow undergoes an inverse transition back to laminar flow beyond the instability zone.

The observation of Mochizuki and Yao [9] that r_c (i.e., the associated critical value of x^*) decreases with increasing Re is in disagreement with the r_c/Re relationship proposed by Peube [16]. In a more recent paper [17] by Mochizuki and Yang, a more comprehensive study of oscillatory flow has been described, and the periodic and alternating formation of vortices at the discs has further been confirmed. There is, in consequence, a critical Re, characteristic of flow separation, for each

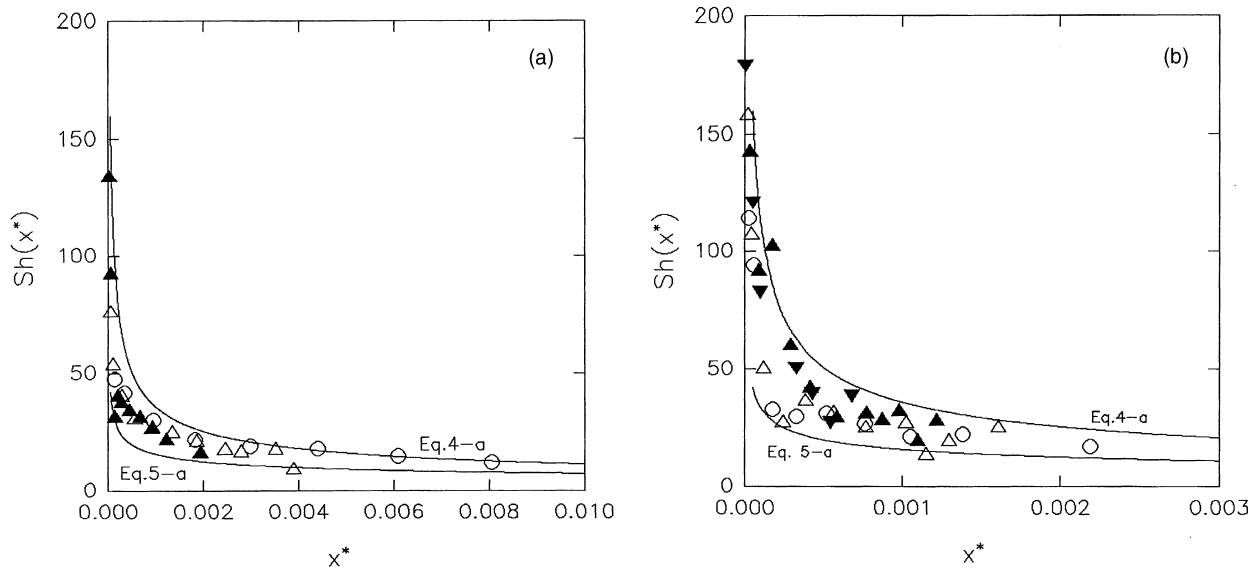

Fig. 7. Variation of the local Sherwood number $Sh(x^*)$ with parameter x^*. (a) $2a = 1.0$ mm; *Re*: (○) 128, (△) 420 and (▲) 840. (b) $2a = 1.6$ mm; *Re*: (○) 294, (△) 398, (▲) 530 and (▼) 945.

value of a/R_1; further, the radial position of flow separation depends exclusively on *Re*, and its numerical value decreases, with increasing *Re*.

Kreith's results on heat transport have been amply considered in papers related to electrochemical applications, in spite of doubts on their theoretical analysis, as outlined in [18]. Kreith's empirical relationships obtained for the sublimation of naphthalene in air ($Sc = 2.4$) [8] are plotted in Figure 6.

Inspection of Figure 6 further indicates that the experimental observations presented in this paper show good agreement with empirical correlations arising from the experiments of Jansson et al. [1, 2, 13]. This finding provides indirect evidence for the correctness of correlating the mean Sherwood number with *Sc*, rather than $Sc^{1/3}$, at least in laminar flow, although the latter has widely been employed in the literature (a comprehensive survey is given in [3]). In others words, an a-priori assumption of the 1/3 exponent for the Schmidt number is not warranted under all experimental conditions.

6. Conclusions

The overall results of this mass transfer study extend the experimental work of Cavalcanti and Cœuret to the laminar flow range and show good agreement with the appropriate analytical solution given by Dworak and Wendt [4] for high Schmidt numbers.

Spatial distributions of local mass flux at the transfer surface agree well with approximate theoretical distributions in the laminar flow regime. This finding validates the applicability of the Dworak–Wendt model [4] beyond its original scope.

Acknowledgements

The authors acknowledge support received from the Natural Sciences and Engineering Research Council of Canada (NSERC) and the *Centre National de la Recherche Scientifique* (CNRS) of France.

References

1. A. Ashworth and R.E.W. Jansson, *Electrochim. Acta* **22** (1977) 1295.
2. J. Ghoroghchian, R.E.W. Jansson and R.J. Marshall, *Electrochim. Acta* **24** (1979) 1175.
3. E. Bezerra Cavalcanti and F. Cœuret, *J. Appl. Electrochem.* **28** (1998) 1419.
4. R. Dworak and H. Wendt, *Ber. Bunsen-Gessellschaft* **80** (1976) 77.
5. R.A. Thomas and M.H. Cobble, *J. Heat Transf.* **85** (1963) 189.
6. F. Kreith, Thèse, Université de Paris (1965).
7. F. Kreith, *Compt. Rend. Acad. Sci. Paris* **260** (1965) 62.
8. F. Kreith, *Int. J. Heat Mass Transf.* **9** (1966) 265.
9. S. Mochizuki and M. Yao, *Trans. Japan Soc. Mech. Eng.* **49** (1983) 426.
10. R. Bird, W.E. Stewart and E.N. Lightfoot, 'Transport Phenomena' (J. Wiley & Sons, New York, 1960), p. 353.
11. R. Bird, W.E. Stewart and E.N. Lightfoot, *op cit.* [10], p. 551.
12. R. Selman and C.W. Tobias, 'Mass transfer measurements by the limiting current technique', *Adv. Chem. Eng.* **10** (Academic Press, New York, 1978), p. 86.
13. S. Ishizawa, *Bull. Jap. Soc. Mech. Eng.* **9** (1985) 377.
14. R.E.W. Jansson and R.J. Marshall, *J. Appl. Electrochem.* **8** (1978) 287.
15. R.V. Shenoy and J.M. Fenton, *Int. J. Heat Mass Transf.* **33** (1990) 2059.
16. J.L. Peube, *J. Mécan. (Paris)* **4** (1963) 377.
17. S. Mochizuki and W.J. Yang, *J. Fluid Mech.* **154** (1985) 377.
18. Z. Fahidy and F. Cœuret, *Can. J. Chem. Eng.*, **79** (2001) 132.